ELSEVIER

Journal of Photochemistry and Photobiology
A: Chemistry 87 (1995) 193–201

Journal of
PHOTOCHEMISTRY
AND
PHOTOBIOLOGY
A:CHEMISTRY

Photoisomerization and adiabatic tautomerization of the α-pyridylpyrrolinones

Frederick D. Lewis *, Beth A. Yoon

Department of Chemistry, Northwestern University, Evanston, IL 60208-3113, USA

Received 1 September 1994; accepted 1 November 1994

Abstract

The spectroscopy and photochemical behavior of *E*- and *Z*-2,3-diethyl-5-(2-pyridylmethylidene)-3-pyrrolin-2-one have been reinvestigated. In accord with earlier reports, *E*,*Z* photoisomerization of the *E* isomer is more efficient than that of the *Z* isomer, resulting in photostationary states enriched in the *Z* isomer. The low reactivity of the *Z* isomer was previously attributed to the presence of an intramolecular hydrogen bond, which is responsible for the greater thermodynamic stability of the *Z* vs. the *E* isomer. The *Z* isomer displays red-shifted fluorescence, attributed to the adiabatic formation of a tautomer which reverts to the *Z* isomer in the ground state. Both the forward (excited state) and reverse (ground state) hydrogen transfer processes have very low activation energies, thus providing a route for the decay of the excited *Z* isomer which competes effectively with isomerization. Short-lived fluorescence attributed to the π,π^* singlet states of both the *E* and *Z* isomers can be observed at 77 K. The short lifetimes may result from rapid internal conversion to lower energy n,π^* states, whose presence is indicated by INDO/S-SCF-CI calculations.

Keywords: One-way isomerization; Intramolecular hydrogen bond; INDO/S calculations; Fluorescence

1. Introduction

The synthesis and photoisomerization of the 3,4-dialkyl-5-(2-pyridylmethylidene)-3-pyrrolin-2-ones **1** and **2** have been reported by several research groups [1–3]. These molecules make up the chromophore of bilirubin and are an integral part of the chromophores of other bile pigments [4]. Thus their photochemistry is of interest with regard to the phototherapy of neonatal jaundice. The greater thermodynamic stability of the *Z* vs. *E* isomer of these molecules is attributed to the existence of an intramolecular hydrogen bond in the *Z* isomer but not the *E* isomer. Hydrogen bonding has also been proposed to influence the efficiency of photoisomerization. Lightner and Park [1] and de Groot et al. [2] attributed their observation of one-way $E \rightarrow Z$ photoisomerization for **2** and **1** respectively in non-hydroxylic solvents to the presence of an intramolecular hydrogen bond in the *Z* isomer. The occurrence of two-way isomerization in methanol solution and for the *N*-methyl analog of **1** was attributed to the disruption or absence of an intramolecular hydrogen bond in the *Z* isomer. Falk and Neufingerl [3] reported the occurrence of the two-way isomerization of **1** in both non-hydroxylic solvents and methanol; however, the quantum yields of isomerization of *Z*-**1** were lower than those of *E*-**1** in all solvents.

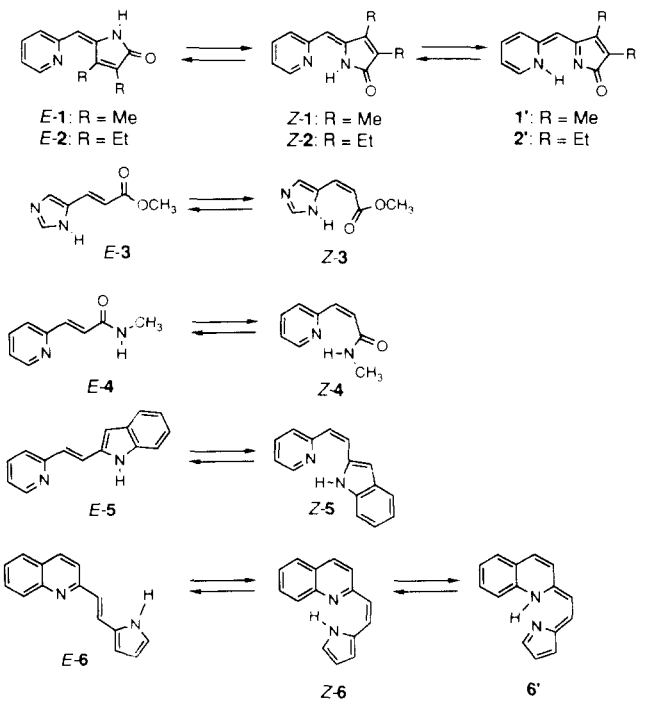

* Corresponding author.

SSDI 1010-6030(94)03988-7

The α-pyridylpyrrolinones are members of a small, but growing, class of molecules in which photoisomerization results in the formation or disruption of an intramolecular hydrogen bond. Other members of this class are shown above and include methyl urocanate **3** and several urocanamides [5], several 3-(2-pyridyl)propenamides **4** [6], pyridylvinylindole **5** [7–9] and 1-(2-pyrrolyl)-2-(2-quinolyl)ethene **6** [10]. One-way $E \rightarrow Z$ photoisomerization is observed for **4** and **5**, whereas two-way isomerization is observed for **3** and **6**. Thus intramolecular hydrogen bonding is not a sufficient condition for the observation of one-way isomerization. In the case of *Z*-**6**, adiabatic intramolecular hydrogen abstraction to form the tautomer **6′** competes with photoisomerization. This observation suggests that the low quantum yields of photoisomerization of the *Z* isomers of **1**–**5** might, in some cases, be a consequence of rapid non-radiative decay involving reversible N–H transfer rather than the existence of an enhanced barrier for isomerization due to intramolecular hydrogen bonding.

In this paper, we report the results of an investigation of the photoisomerization and spectroscopy of *E*-**2** and *Z*-**2**. On the basis of these results, we propose that the low efficiency of isomerization of the thermodynamically more stable isomer *Z*-**2** is a consequence of adiabatic hydrogen transfer to form a fluorescence tautomer **2′** which rapidly reverts to *Z*-**2** in the ground state (see above). The less stable isomer *E*-**2** undergoes efficient isomerization to form *Z*-**2** at room temperature and even in a 77 K glass. The nature of the excited states involved in these transformations has been investigated using INDO/S-SCF-CI calculations.

2. Experimental details

Proton nuclear magnetic resonance (^{1}H NMR) spectra were recorded on a Gemini 300 MHz spectrophotometer in $CDCl_3$ with tetramethylsilane (TMS) as internal standard. UV–visible absorption spectra were measured with a Hewlett-Packard model 8452A diode array spectrophotometer in quartz cuvettes (path length, 1 cm). Room temperature emission and excitation spectra of solutions stoppered with white rubber septa (Aldrich) and purged with nitrogen for more than 5 min were recorded using a Spex FluoroMax spectrophotometer in quartz cells (path length, 1 cm). Fluorescence quantum yields were determined relative to *trans*-stilbene ($\Phi_f = 0.05$ in methylcyclohexane) [11]. Solutions with concentrations of approximately 10^{-4} M were purged with nitrogen for more than 5 min in quartz cuvettes or quartz electron paramagnetic resonance (EPR) tubes (0.5 cm o.d.). Fluorescence lifetimes were measured with a PTI LS-1 spectrophotometer using a gated hydrogen arc lamp and single-photon-counting techniques. The decays were deconvoluted using a single multiexponential least-squares analysis. The reduced χ^2 values, randomness of the residuals and autocorrelation functions were used to determine the goodness of the fit. Low temperature emission spectra and fluorescence lifetimes were obtained using a liquid nitrogen- cooled fluorescence Dewar with a hanging finger window or an Oxford Instruments variable temperature liquid nitrogen cryostat (model DN1704) equipped with a temperature controller (model ITC4).

The light source for photostationary state measurements was a Hanovia 450 W high pressure mercury arc lamp with merry-go-round apparatus; Corning glass filters 7-54 and 0-52 (366 nm) and a potassium chromate filter solution (313 nm) were used. The light source for quantum yield measurements was an optical bench equipped with a 200 W high pressure Oriel mercury–xenon lamp, a Bausch and Lomb high intensity monochromator and a thermostatically controlled cell holder with a magnetic stirrer.

Photochemical equilibria and quantum yields were determined in triplicate for 2 ml aliquots of solutions of approximately 10^{-4} M contained in quartz cuvettes. Solutions were purged for more than 5 min with dry nitrogen prior to irradiation and stirred during irradiation. The UV spectra of standard solutions of *E*-**2** and *Z*-**2** at varying concentrations were recorded and saved. The isomer composition of irradiated solutions was determined by comparing observed spectra with calibration curves calculated by Hewlett-Packard Quant II software. Quantum yields were determined at less than 10% conversion using 313 nm irradiation with *trans*-stilbene isomerization as the actinometer [12]. Aberchrome 540 was used as an actinometer at 366 nm [13]. Thermal isomerization of *E*-**2** to *Z*-**2** precluded gas chromatography (GC) analysis; therefore conversion ratios were determined using UV spectroscopy. Photodegradation of *E*-**2** and *Z*-**2** was not observed even in dilute solutions (10^{-5} M).

INDO/S-SCF-CI (ZINDO) calculations were performed using the method developed by Zerner and coworkers [14] and implemented as described by Lewis et al. [15]. The geometries for *E*-**1**, *Z*-**1** and **1′** were assumed to be the minimum energy conformation as described by MM2 [16] or MAXIMIN2 [17]. The ZINDO calculations were performed on a Stellar mini-supercomputer and required approximately 5–10 min of CPU time.

Solvents were of spectral grade (Aldrich or Fisher). Dichloromethane was distilled over calcium hydride prior to use. Methanol (MeOH) was used as received. Dimethylsulfoxide (DMSO) was distilled over $NaNH_2$. *trans*-Stilbene (Aldrich) was recrystallized twice from benzene and once from ethanol. All other compounds were used as received. *Z*-3,4-Diethyl-5-(2-pyridylmethylidene)-3-pyrrolin-2-one (*Z*-**2**) was prepared by the

method of Lightner and Park [1]: melting point (m.p.), 61–65 °C (63–64 °C [1]). A solution of 0.01 M *Z*-**2** in methanol under an N_2 atmosphere was irradiated (366 nm) until optimum conversion to *E*-**2** was obtained (approximately 52%). Removal of the solvent followed by preparative thin layer chromatography (5% methanol in chloroform) yielded *E*-**2**: m.p., 100–103 °C (95–97 °C [1]). Analysis by GC revealed the absence of impurities other than *Z*-**2**, and integration of the ^{1}H NMR spectrum indicated the presence of 2% *Z*-**2**.

3. Results

3.1. Photoisomerization

The quantum yields of photoisomerization of *E*-**2** and *Z*-**2**, determined using monochromatic 313 nm irradiation in several solvents, are summarized in Table 1. Due to the occurrence of thermal $E \rightarrow Z$ isomerization under the conditions of GC analysis, the extent of isomerization was determined at low conversion (approximately 10%) using UV spectroscopy. Accurate analysis of isomer mixtures by UV spectroscopy is possible due to the difference in the absorption spectra of the *E* and *Z* isomers (see below) and the absence of competing photoprocesses even following prolonged irradiation. The values of $\Phi_{E,Z}$ are large (about 0.5) and independent of solvent polarity, while the values of $\Phi_{Z,E}$ are smaller and decrease with increasing solvent polarity. The values measured in methanol solution are similar to those obtained by Falk and Neufingerl [3] for 330 nm irradiation of **1** in the same solvent.

The photostationary states obtained from the irradiation of *E*-**2** and *Z*-**2** in several solvents using monochromatic 313 nm or 365 nm light are also reported in Table 1. The observed photostationary states for 313 nm irradiation are in good agreement with the values calculated from the measured quantum yields and molar absorbance, both of which are solvent dependent. The photostationary states obtained using 365 nm irradiation contain a higher percentage of the *E* isomer due to the more selective absorption of light by the *Z* isomer at this wavelength than at 313 nm. Falk and Neufingerl [3] reported photostationary states for the 300 nm irradiation of **1** consisting of 30% and 29% of the *E* isomer in chloroform and methanol solution respectively. These values are intermediate between those obtained for **2** using 313 nm and 365 nm irradiation in dichloromethane and methanol solutions respectively (Table 1). Lightner and Park [1] reported photostationary states for the irradiation of **2** with a quartz-filtered mercury arc lamp consisting of 10% and 18% of the *E* isomer in DMSO and methanol solution respectively. Curiously, they observed no photoisomerization of *Z*-**2** in chloroform or tetrahydrofuran solution. The use of short-wavelength irradiation may have generated low concentrations of free radicals or acid catalysts capable of initiating thermal $E \rightarrow Z$ isomerization in these solvents.

Table 1
Photoisomerization data for (*E*)- and (*Z*)-2,3diethyl-5-(2-pyridylmethylidene)-3-pyrrolin-2-one

Solvent	$\Phi_{E,Z}$ [a]	$\Phi_{Z,E}$ [a]	E_{365} [b] (%)	E_{365} [c] (%)
CH_2Cl_2	0.50	0.16	14	46
MeOH	0.44	0.08	15	52
DMSO	0.48	0.038	<3	23

[a] Quantum yield of photoisomerization using 313 nm light.
[b] Photostationary state obtained using 313 nm light.
[c] Photostationary state obtained using 365 nm light.

3.2. Molecular structure and spectra

The existence of an intramolecular hydrogen bond in *Z*-**1** and *Z*-**2** is indicated by the lower IR N–H stretching frequency for the *Z* vs. *E* isomer. Falk and Neufingerl [3] concluded, on the basis of lanthanide-induced shift measurements, that *Z*-**1** is an essentially planar molecule, whereas *E*-**1** is non-planar, with a dihedral angle of approximately 35° between the pyridine and pyrrolinone chromophores. This large dihedral angle is necessary to relieve non-bonded repulsion between the C-4 methyl and pyridine ring. The MM2 minimized structures of *Z*-**1** and *E*-**1**, shown in Fig. 1, are compatible with these results. The calculated struc-

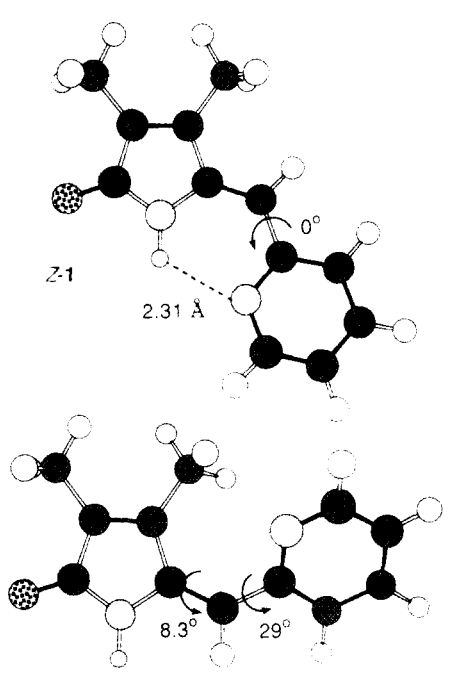

Fig. 1. MM2 minimum energy conformations of *E*- and *Z*-3,4-dimethyl-5-(2-pyridylmethylidene)-3-pyrrolin-2-one.

ture for *Z*-**1** is planar with an intramolecular N–H···N distance of 2.31 Å. This distance is somewhat longer than the calculated N–H···O distance in the planar *Z*-**3** molecule (2.06 Å) [5] and the calculated N–H···N distance in the non-planar *Z*-**4** molecule (2.19 Å) [6]. The calculated structure for *E*-**1** has a somewhat smaller pyridyl–vinyl dihedral angle (29°) than that calculated by Falk and Neufingerl [3] and a small torsional angle (8°) about the exocyclic double bond. Rotation by approximately 180° about the pyridyl–vinyl bond in *Z*-**1** leads to a higher energy rotamer lacking an intramolecular hydrogen bond, whereas rotation in *E*-**1** yields a rotamer with increased steric energy. The MAXIMIN2 minimized structure of **1′** is planar with an intramolecular N–H···N distance of 2.28 Å, slightly shorter than that calculated for *Z*-**1**.

The calculated energy difference between *Z*-**1** and *E*-**1** is 3.3 kcal mol^{-1}. This value is similar to the strength of the intramolecular hydrogen bond estimated by Falk and Neufingerl [3] (approximately 4 kcal mol^{-1}) on the basis of IR frequency shifts, and is consistent with the observation of a single isomer, *Z*-**1**, under conditions of thermal equilibrium. *N*-Methylation of **1** results in a much smaller energy difference between the isomers, as indicated by a *Z*-**1** : *E*-**1** ratio of 3 : 2 at thermal equilibrium [2].

The electronic absorption spectra of *Z*-**2** and *E*-**2** in dichloromethane solution are shown in Fig. 2. These spectra are similar in appearance to those reported for *Z*-**1** and *E*-**1** in ethanol solution. The absorption spectral data for *Z*-**2** and *E*-**2** in several solvents are summarized in Table 2. The lowest energy absorption band of *E*-**2** is shifted to lower energy in more polar solvents, whereas the absorption spectrum of *Z*-**2** is relatively insensitive to the solvent polarity. Similar solvent effects have been reported for *Z*-**1** and *E*-**1** [3]. The different effects of solvent polarity on the *E* vs. *Z* isomer may reflect the presence of the intramolecular hydrogen bond in *Z*-**2**, which reduces the effective polarity of the molecule and its interaction with polar solvents. The solvation of *E*-**2** may affect the pyridyl–vinyl dihedral angle as well as the energies of the non-bonding orbitals (see below).

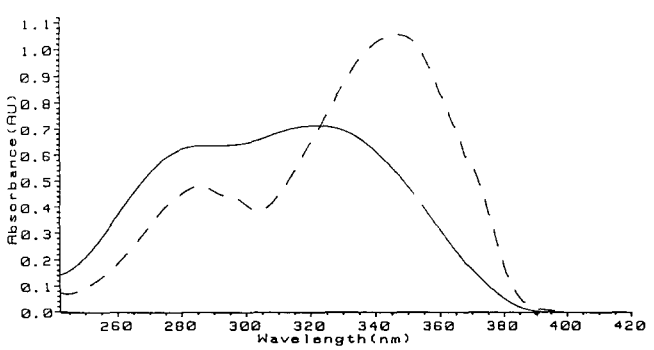

Fig. 2. UV spectra of 5.0×10^{-5} M *E*- (full line) and *Z*-3,4-diethyl-5-(2-pyridylmethylidene)-3-pyrrolin-2-one (broken line) in dichloromethane solution.

Table 2
UV absorption data for (*E*)- and (*Z*)-3,4-diethyl-5-(2-pyridylmethylidene)-3-pyrrolin-2-one [a]

Isomer	Solvent	λ_{max}	ϵ (λ_{max})
Z-**2**	CH_2Cl_2	286, 346	9600, 25100
	MeOH	282, 344	10400, 26500
	DMSO	286, 350	9800, 23600
E-**2**	CH_2Cl_2	284, 322	12600, 14200
	MeOH	284 [b]	14100 [b]
	DMSO	286, 336	13000, 16400

[a] Data for $(2.5–50.0) \times 10^{-5}$ M solutions.
[b] Longer wavelength band unresolved.

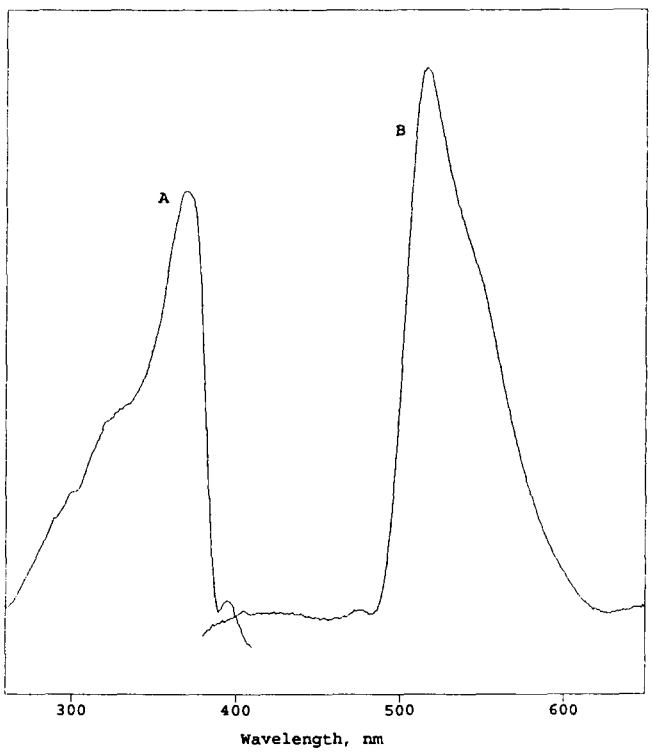

Fig. 3. Emission (A) and excitation (B) spectra of *Z*-3,4-diethyl-5-(2-pyridylmethylidene)-3-pyrrolin-2-one in dichloromethane solution at room temperature; $\lambda_{ex} = 360$ nm; $\lambda_{em} = 520$ nm.

The fluorescence emission and excitation spectra of *Z*-**2** in dichloromethane solution at room temperature are shown in Fig. 3. The fluorescence is substantially red shifted with respect to the absorption and fluorescence excitation spectra and is assigned to the tautomer **2′**. The fluorescence quantum yield is 0.02 in methylcyclohexane solution. Values of Φ_f decrease with increasing solvent polarity; however, the emission maximum is not sensitive to the solvent polarity. The fluorescence decay times determined by time-correlated single-photon counting in methylcyclohexane and methyltetrahydrofuran solution are 0.7 ns and 0.3 ns re-

spectively. The fluorescence observed for *E*-**2** at room temperature in methylcyclohexane solution is identical to that observed for *Z*-**2**, and is attributed to the *Z*-**2** impurity present in our sample of *E*-**2** (approximately 2%).

The fluorescence emission and excitation spectra of *Z*-**2** in an EPA (ethanol:isopentane:ether 2:5:5) glass at 77 K are shown in Fig. 4. Two emission bands are observed under these conditions: a low energy band similar to that observed at room temperature (λ_{max} = 518 nm) and a higher energy band (λ_{max} = 400 nm). These bands display similar poorly resolved vibrational structure ($\Delta\nu$ = 1160 cm^{-1}) and essentially identical excitation spectra. The 380 nm band observed in the excitation spectrum is also observed in the low temperature absorption spectrum and appears as a shoulder in the room temperature absorption spectrum at higher concentrations. The ratio of the 400 nm to 518 nm fluorescence intensity increases with increasing solvent polarity from about 1 : 7 in methylcyclohexane to 1 : 3 in methyltetrahydrofuran and 1 : 2 in EPA. The decay time of the 400 nm fluorescence is shorter than the time resolution of our instrumentation (approximately 0.2 ns), while the decay time of the 518 nm fluorescence is longer at 77 K than at room temperature (1.5 ns vs. 0.3 ns in methyltetrahydrofuran).

The fluorescence emission and excitation spectra of *E*-**2** in an EPA glass at 77 K are shown in Fig. 5. The low energy emission band and its excitation spectrum and fluorescence lifetime are identical to those of *Z*-**2**; however, the high energy band (λ_{max} = 420 nm) and its excitation spectrum are broader than those of the 400 nm band of *Z*-**2**. Furthermore, the ratio of the 420 nm to 518 nm fluorescence for *E*-**2** is relatively insensitive to the solvent polarity. Thus we conclude that the 420 nm emission originates from *E*-**2**. The weaker 518 nm emission most probably originates from *Z*-**2** present as an impurity in the sample of *E*-**2**. Irradiation of *E*-**2** in a methylcyclohexane glass at 77 K results in conversion to *Z*-**2**, as indicated by changes in the absorption and fluorescence spectra. The quantum yield of isomerization was not measured; however, the isomerization process appears to be relatively efficient even at 77 K.

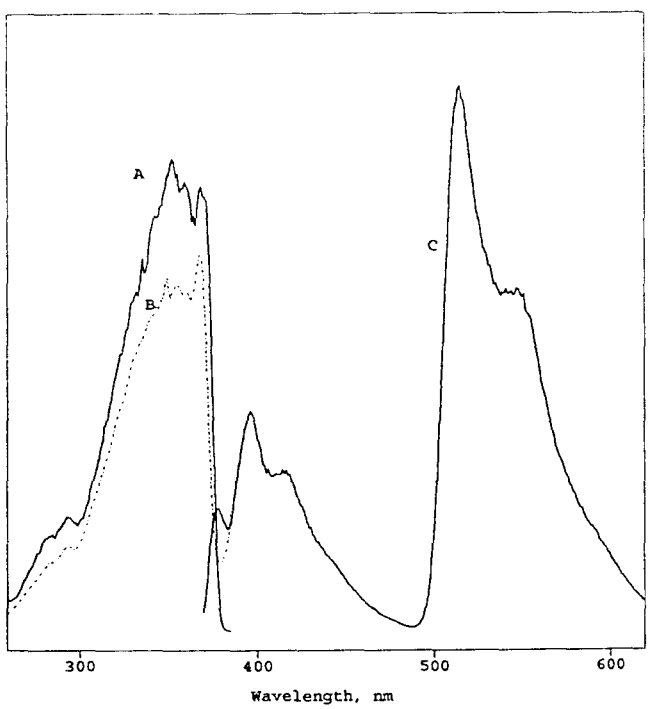

Fig. 4. Emission and excitation spectra of *Z*-3,4-diethyl-5-(2-pyridylmethylidene)-3-pyrrolin-2-one in an EPA glass at 77 K; λ_{em} = 520 nm (A); λ_{em} = 400 nm (B); λ_{ex} = 360 nm (C).

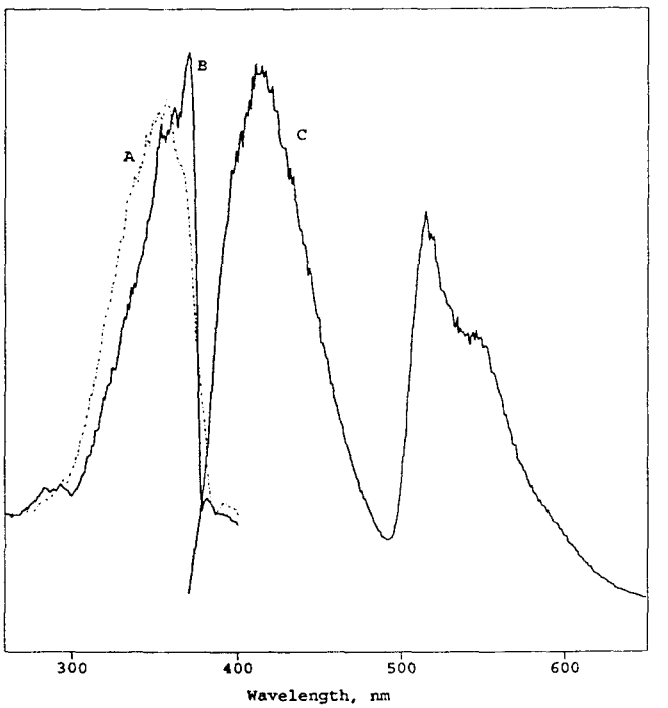

Fig. 5. Emission and excitation spectra of *E*-3,4-diethyl-5-(2-pyridylmethylidene)-3-pyrrolin-2-one in an EPA glass at 77 K; λ_{em} = 420 nm (A); λ_{em} = 520 nm (B); λ_{ex} = 360 nm (C).

3.3. ZINDO calculations

The lowest energy absorption bands in *Z*-**1** and *E*-**1** have been assigned to π,π^* transitions on the basis of PPP (LCAO-SCF-CI) calculations [3]. The higher energy and smaller oscillator of *E*-**1** vs. *Z*-**1** was attributed to the non-planarity of *E*-**1**. We have investigated the electronic structure and spectra of *Z*-**1**, *E*-**1** and **1'** (the dimethyl analog of **2'**) by means of semiempirical INDO/S-SCF-CI (ZINDO) calculations using the algorithm developed by Zerner and coworkers [14]. The molecular structures were calculated using MM2 (*Z*-**1** and *E*-**1**) or MAXIMIN2 (**1'**). The ZINDO-derived frontier molecular orbitals and orbital energies for *Z*-**1** and *E*-**1** are shown in Fig. 6. The most interesting feature of

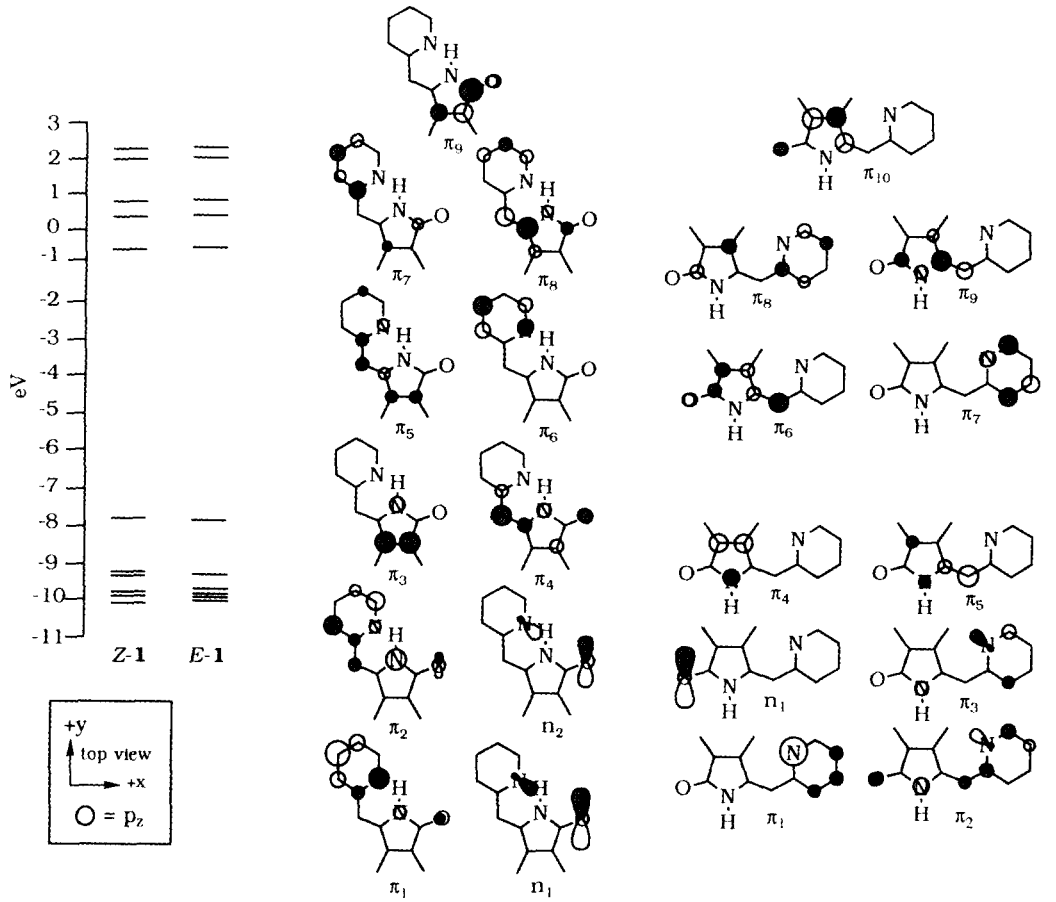

Fig. 6. ZINDO calculated molecular orbitals for *E*- and *Z*-3,4-dimethyl-5-(2-pyridylmethylidene)-3-pyrrolin-2-one.

these orbitals is the appearance of the non-bonding orbitals. In the case of *Z*-**1**, there are two n orbitals (n_1 and n_2), resulting from the symmetric and antisymmetric combination of the carbonyl and pyridine non-bonding orbitals, whereas in *E*-**1** the highest occupied n orbital is localized on the carbonyl. The location of the non-bonding orbitals below the highest energy filled π orbitals is consistent with the ordering of the ionization energies in the photoelectron spectrum of 2-vinylpyridine [18].

The calculated absorption maxima, oscillator strengths and character of selected excited singlet states of *Z*-**1**, *E*-**1** and **1′** are reported in Table 3. The lowest energy allowed transition for all three isomers is a relatively pure highest occupied molecular orbital (HOMO) to lowest unoccupied molecular orbital (LUMO) $\pi \rightarrow \pi^*$ transition (S_3 for *Z*-**1** and *E*-**1** and S_2 for **1′**). Two additional $\pi \rightarrow \pi^*$ transitions with more extensive configuration interaction and lower oscillator strengths are predicted to lie at higher energy. The calculated energies of these transitions are in reasonable agreement with the observed spectra (Figs. 2 and 3). ZINDO also predicts the presence of low energy $n \rightarrow \pi^*$ transitions with extensive configuration interaction and low oscillator strengths. These low energy singlet states are not observed in the electronic absorption spectra, but may be obscured by the broad, allowed $\pi \rightarrow \pi^*$ transitions. These calculations have been performed for vertical excited states. Twisting about the C=C bond or other geometrical changes will, no doubt, result in changes in the energies of the excited singlet states.

4. Discussion

The photoisomerization of **1** and several related molecules was proposed by Falk and Neufingerl [3] to occur via a singlet excited state on the basis of sensitization and quenching experiments. A potential energy surface for the singlet state isomerization of **1** and **2**, based on that for stilbene and other aryl olefins [19], is shown in Fig. 7 (left side). Reversal of the normal thermodynamic preference for *E* vs. *Z* isomers is a consequence of the non-bonded repulsion in *E*-**2** and the presence of an intramolecular hydrogen bond in *Z*-**2**. Singlet energies of approximately 75 kcal mol^{-1} for the lowest energy singlet π,π^* states can be estimated from the low temperature fluorescence spectra of *Z*-**2** and *E*-**2**. Thus both the ground state and the lowest π,π^* singlet state of *Z*-**2** are about 4 kcal mol^{-1} lower

Table 3
Calculated absorption maxima (λ_{max}), oscillator strengths (f) and configuration interaction (CI) of excited singlet states (S) of (*E*)- and (*Z*)-3,4-dimethyl-5-(2-pyridylmethylidene)-3-pyrrolin-2-one and the tautomer of (*Z*)-3,4-dimethyl-5-(2-pyridylmethylidene)-3-pyrrolin-2-one

Isomer	Excited state	λ_{max} (nm) (f)	CI (%) and character
E-**1**	S_1	352 (0.001)	62% $n_1 \rightarrow \pi_6$
			10% $n_1 \rightarrow \pi_9$
			14% $n_2 \rightarrow \pi_{10}$
	S_3	306 (0.904)	74% $\pi_5 \rightarrow \pi_6$
	S_4	276 (0.146)	13% $\pi_3 \rightarrow \pi_6$
			49% $\pi_5 \rightarrow \pi_7$
	S_5	268 (0.118)	14% $\pi_2 \rightarrow \pi_6$
			64% $\pi_4 \rightarrow \pi_6$
Z-**1**	S_1	361 (0.002)	18% $n_1 \rightarrow \pi_5$
			48% $n_2 \rightarrow \pi_5$
	S_3	322 (0.783)	85% $\pi_4 \rightarrow \pi_5$
	S_4	277 (0.240)	10% $\pi_2 \rightarrow \pi_5$
			59% $\pi_4 \rightarrow \pi_6$
	S_5	273 (0.083)	10% $\pi_2 \rightarrow \pi_5$
			74% $\pi_3 \rightarrow \pi_5$
1′	S_1	532 (0.001)	69% $n_1 \rightarrow \pi_3$
			17% $n_1 \rightarrow \pi_4$
	S_2	460 (0.382	81% $\pi_2 \rightarrow \pi_3$
	S_3	388 (0.172)	52% $\pi_1 \rightarrow \pi_3$
			13% $\pi_2 \rightarrow \pi_3$
			21% $\pi_2 \rightarrow \pi_4$
	S_4	350 (0.451)	14% $\pi_1 \rightarrow \pi_3$
			74% $\pi_2 \rightarrow \pi_4$

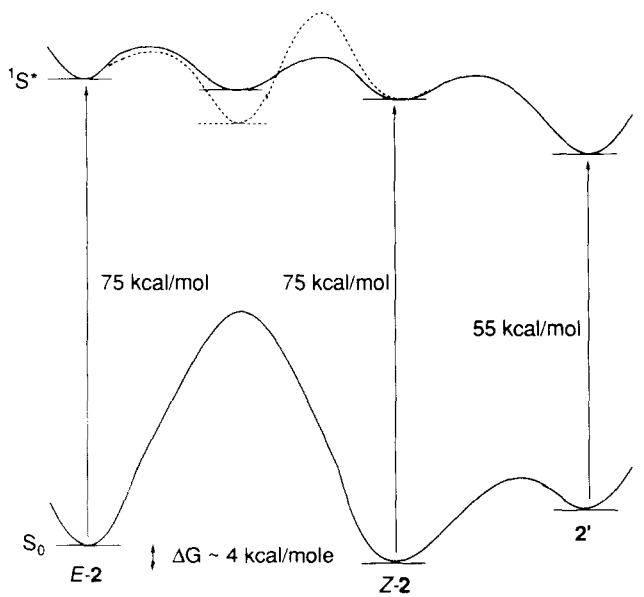

Fig. 7. Schematic potential energy surfaces for the singlet state photoisomerization and hydrogen transfer of 3,4-diethyl-5-(2-pyridylmethylidene)-3-pyrrolin-2-one with the energy of the twisted intermediate above (full line) or below (broken line) that of the *Z* isomer.

than those of the *E* isomer. The high quantum yield of isomerization of *E*-**2** (Table 1) is indicative of a low barrier for torsion about the double bond to yield a twisted intermediate which can decay to yield both *E*-**2** and *Z*-**2**. The low quantum yield of isomerization of *Z*-**2** is responsible for the high *Z* isomer content of steady state isomer mixtures (Table 1). The inefficient isomerization of *Z*-**2** might result from a large barrier for torsion (Fig. 7, broken curve), endergonic torsion (Fig. 7, full curve) or competing intramolecular hydrogen transfer (Fig. 7, right side).

The large Stokes shift for the fluorescence of *Z*-**2** (Fig. 3) is similar to that reported by Arai et al. [10] for *Z*-**6** and assigned to the fluorescent tautomer **6′**. By analogy, the 518 nm fluorescence of *Z*-**2** can be assigned to the tautomer **2′** formed via intramolecular hydrogen transfer. The 400 nm fluorescence observed for *Z*-**2** at 77 K (Fig. 4) bears the expected mirror image relationship to the absorption and fluorescence excitation spectra of *Z*-**2** and is assigned to the singlet state of *Z*-**2**. There is no evidence for the accumulation of ground state **2′** (see below), and thus the 518 nm fluorescence observed from *Z*-**2** must result from an adiabatic hydrogen transfer process which yields the fluorescent singlet state of **2′**. Since this process occurs even at 77 K, the barrier for singlet state hydrogen transfer must be very small. The increase in the 400 nm fluorescence in polar vs. non-polar glasses indicates that the hydrogen transfer process is slower in polar glasses. This could reflect a larger solvent reorganization energy for hydrogen transfer in the more polar medium.

Once formed, the singlet state of **2′** can decay to the ground state via fluorescence or non-radiative decay. The low fluorescence quantum yield ($\Phi_f = 0.02$) indicates that either the quantum yield for the adiabatic hydrogen transfer process is low or non-radiative decay of singlet **2′** is more rapid than fluorescence. The fluorescence decay times of **2′** are similar at 77 K and room temperature in both methylcyclohexane (0.7 ns at both temperatures) and methyltetrahydrofuran (1.4 ns vs. 0.3 ns). Thus non-radiative decay of singlet **2′** cannot be activated. Arai et al. [10] have detected **6′** and measured a decay time of 300 ns by means of transient absorption spectroscopy. ZINDO calculations indicate that **2′** should have an allowed absorption band at 460 nm (Table 3); however, excitation at this wavelength after continuous irradiation of *Z*-**2** at 77 K does not result in the observation of 518 nm fluorescence. Our attempts to detect an intermediate absorbing in the 400–500 nm region via nanosecond time-resolved absorption spectroscopy have been unsuccessful. Thus we conclude that the barrier for ground state reversion of **2′** to *Z*-**2**, like that for excited state hydrogen transfer, is very small.

The fluorescence behavior of *Z*-**2** can be rationalized using a reversed asymmetric potential energy surface

[20] (Fig. 7, right side) similar to that proposed by Arai et al. [10] for *Z*-**6**. If the ground state energy difference between *Z*-**2** and **2′** is assumed to be one-half of the difference in the fluorescence energies, as shown in Fig. 7, then both forward and return hydrogen transfer would be exergonic by approximately 10 kcal mol^{-1}. The energy of **2′** could be shifted either up or down by several kilocalories per mole with respect to that of *Z*-**2** without affecting the necessary condition of exergonic forward (excited state) and reverse (ground state) hydrogen transfer.

The 420 nm emission observed for *E*-**2** at 77 K (Fig. 5) is attributed to the fluorescence of *E*-**2**. The absence of vibrational structure in both the fluorescence emission and excitation spectra is consistent with the non-planar structure of *E*-**2** (Fig. 1). The weaker 518 nm emission is attributed to the excitation of *Z*-**2** present as an impurity, on the basis of its excitation spectrum, which is identical to that of *Z*-**2** fluorescence at 77 K (Fig. 5). Irradiation of *E*-**2** at 77 K results in the appearance of a structured fluorescence similar to that of *Z*-**2** and an increase in the intensity of the 518 nm emission. If isomerization and fluorescence of *E*-**2** at 77 K occur via the same singlet state, the barrier for isomerization of *E*-**2** must be exceptionally low. Singlet *cis*-stilbene, which has no intrinsic barrier for isomerization, does not undergo isomerization at 77 K and has a singlet lifetime of 1.4 ns in a 3-methylpentane glass [21]. Greater non-bonded repulsion in *E*-**2** vs. *cis*-stilbene could account for this difference in behavior.

Although we have attributed the low temperature fluorescence of *Z*-**2** and *E*-**2** (Figs. 4 and 5) and the lowest energy allowed absorption bands (Fig. 2) to HOMO→LUMO $\pi \rightarrow \pi^*$ transitions, ZINDO calculations indicate that forbidden $n \rightarrow \pi^*$ transitions lie at lower energies than the allowed $\pi \rightarrow \pi^*$ transitions (Table 3). The forbidden nature of the $n \rightarrow \pi^*$ transitions could account for our inability to detect their presence spectroscopically. The involvement of an n,π^* state in the hydrogen abstraction process of *Z*-**2** is highly plausible in view of the N–H bonding nature of the n orbitals (Fig. 6). The n,π^* states of aromatic ketones are well known to be more reactive towards hydrogen abstraction than their π,π^* states [22]. Thus internal conversion of the initially populated π,π^* singlet state to an n,π^* state could account for the very short lifetime of the low temperature fluorescence assigned to the π,π^* singlet state of *Z*-**2** and *E*-**2** as well as the formation of **2′** from *Z*-**2**. The involvement of n,π^* states in *E*,*Z* photoisomerization appears less likely than the involvement of π,π^* states. Hence the inefficient photoisomerization of *Z*-**2** might occur from the initially populated singlet π,π^* state or from a triplet π,π^* state formed via intersystem crossing. Similarly, the efficient isomerization of *E*-**2** could occur via either a singlet or triplet π,π^* state. Barrier-less triplet isomerization (as observed for other aryl olefins) could account for the isomerization of *E*-**2** at 77 K and for previous failures to quench the isomerization of *E*-**1** and related molecules with triplet quenchers.

Thus we can conclude that the low quantum yield for the photoisomerization of *Z*-**2** is a consequence of the competing adiabatic hydrogen transfer which yields the fluorescent tautomer **2′**. The ground state of **2′** reverts rapidly to *Z*-**2**. While the low temperature fluorescence of *E*-**2** and *Z*-**2** can be assigned with confidence to the π,π^* singlet states, it is possible that these are upper singlet states which decay rapidly to lower energy n,π^* states. Thus the identities of the excited states involved in the isomerization and tautomerization processes remain to be assigned.

Acknowledgements

Acknowledgement is made to the Donors of the Petroleum Research Fund, administered by the American Chemical Society, for support of this research. We thank Laba Karki for assistance with the transient absorption measurements.

References

[1] D.A. Lightner and Y.-T. Park, *J. Heterocycl. Chem., 14* (1977) 415.
[2] J.A. de Groot, H. Jansen, J.R. Fokkens and J. Lugtenburg, *Recl. Trav. Chim. Pays-Bas, 102* (1983) 114.
[3] H. Falk and F. Neufingerl, *Monatsh. Chem., 110* (1979) 1243.
[4] D.A. Lightner and A.F. McDonagh, *Acc. Chem. Res., 17* (1984) 417.
[5] F.D. Lewis, D.K. Howard, J.D. Oxman, A.L. Upthagrove and A.L. Quillen, *J. Am. Chem. Soc., 108* (1986) 5964; F.D. Lewis and B.A. Yoon, *Res. Chem. Intermed.*, in press.
[6] F.D. Lewis, C.L. Stern and B.A. Yoon, *J. Am. Chem. Soc., 114* (1992) 3131; F.D. Lewis and B.A. Yoon, *J. Org. Chem., 59* (1994) 2537.
[7] J.A. Eenkhoorn, S.O. de Silva and V. Snieckus, *Can. J. Chem., 51* (1972) 792.
[8] T. Arai, T. Iwasaki and K. Tokumaru, *Chem. Lett.*, (1993) 691.
[9] F.D. Lewis, B.A. Yoon, T. Arai, T. Iwasaki and K. Tokumaru, *J. Am. Chem. Soc.*, in press.
[10] T. Arai, M. Moriyama and K. Tokumaru, *J. Am. Chem. Soc., 116* (1994) 3171.
[11] J. Saltiel and J.T. D'Agostino, *J. Am. Chem. Soc., 94* (1972) 6445.
[12] F.D. Lewis and D.E. Johnson, *J. Photochem., 7* (1977) 421.
[13] H.G. Heller and J.R. Langar, *J. Chem. Soc., Perkin Trans., 2* (1981) 341.
[14] A.D. Bacon and M.C. Zerner, *Theor. Chim. Acta, 53* (1970) 21; M.C. Zerner, G.H. Loew, R.R. Kirchner and U.T. Mueller-Westerhoff, *J. Am. Chem. Soc., 102* (1980) 589; J. Ridley and M. Zerner, *Theor. Chim. Acta, 3* (1973) 111; W.P. Anderson, W.D. Edwards and M.C. Zerner, *Inorg. Chem., 25* (1986) 2728.

[15] F.D. Lewis, G.D. Salvi, D.R. Kanis and M.A. Ratner, *Inorg. Chem.*, *32* (1993) 1251.
[16] U. Burkert and N.L. Allinger, *Molecular Mechanics, ACS Monograph Series 117*, American Chemical Society, Washington DC, 1982; C.E. Kundrot, J.W. Ponder and F.M. Richards, *J. Comput. Chem.*, *12* (1991) 402.
[17] MAXIMIN2, Sybyl, Tripos Associates, St. Louis, MO, USA.
[18] A. Modelli and F. Distefano, *J. Electron Spectrosc. Relat. Phenom.*, *23* (1981) 323.
[19] J. Saltiel and Y.-P. Sun, in H. Dürr and H. Bouas-Laurent (eds.), *Photochromism, Molecules and Systems*, Elsevier, Amsterdam, 1990, p. 64; D.H. Waldeck, *Chem. Rev.*, *91* (1991) 415.
[20] P.F. Barbara, P.K. Walsh and L.E. Brus, *J. Phys. Chem.*, *93* (1989) 29.
[21] K. Yoshihara, A. Namiki, M. Sumitani and N. Nakashima, *J. Chem. Phys.*, *70* (1979) 2892.
[22] P.J. Wagner, *Acc. Chem. Res.*, *4* (1971) 168.